

# We are IntechOpen, the world's leading publisher of Open Access books Built by scientists, for scientists

6,900

Open access books available

186,000

International authors and editors

200M

Downloads

Our authors are among the

154

Countries delivered to

TOP 1%

most cited scientists

12.2%

Contributors from top 500 universities



WEB OF SCIENCE™

Selection of our books indexed in the Book Citation Index  
in Web of Science™ Core Collection (BKCI)

Interested in publishing with us?  
Contact [book.department@intechopen.com](mailto:book.department@intechopen.com)

Numbers displayed above are based on latest data collected.  
For more information visit [www.intechopen.com](http://www.intechopen.com)



# Investigation of the Production of Medical Ir-192 Used in Cancer Therapy via Particle Accelerator

*Ozan Artun*

## Abstract

To investigate the production of medical Ir-192 radionuclide used in brachytherapy on Os targets in the energy range of  $E_{\text{particle}} = 100 \rightarrow 1$  MeV, we calculated the cross-section results for charged particle-induced reactions. The calculation was done via TALYS code and simulated activity and yield of product of each reaction process in the irradiation time of 1 h with constant beam current of 1  $\mu\text{A}$ . The calculated results were compared with experimental data in the literature. Moreover, based on the calculated cross-section data and the mass stopping powers obtained from X-PMSP program, the integral yield results of all the reaction processes to produce Ir-192 on Os targets were presented as a function of incident particle energy. The obtained results were discussed to recommend appropriate reaction processes and targets for the production of Ir-192.

**Keywords:** particle accelerator, cancer therapy, radioisotope production, yield, irradiation

## 1. Introduction

Particle accelerators and colliders are widespread ranging from radioisotope production for medical subjects to exploration of new particles in the high physics. For this aim, different collider and accelerator systems have been established by research intuitions and organizations across the world based on powerful accelerators. In general, the largest particle accelerators (in TeV) are used for elementary particle physics to research subatomic particles in physics such as Fermilab or Large Hadron Collider (LHC) at CERN. Additionally, investigating the structure of nuclei in GeV and researching isotopes in nuclear physics have been performed by Relativistic Heavy Ion Collider (RHIC) at the Brookhaven National Laboratory and Los Alamos Neutron Science Center (LANSCE) at Los Alamos. At lower energies, accelerators used in medicine have vital importance in terms of treatment of cancer and diagnosis aims of cancer tissues, especially for the production of medical radioisotopes in MeV. That's why, for an application of particle accelerators, this chapter gives the production of medical iridium-192 used in brachytherapy via particle accelerator.

The iridium-192 that can be used in brachytherapy with interstitial implantation by irradiating malignant tumors is important for therapeutic aims especially for the brain, uterus, head, etc. [1] because the radioisotope Ir-192 with low-energy and high-intensity beta radiation has effective decay properties, which are  $T_{1/2} = 78.83$  d,

EC = 5%,  $I_{\beta^-}$  = 95%, and  $E_{\beta^-}$  = 7 MeV, for using in medical applications [2]. Therefore, the production of such a radioisotope is fairly attractive, and there are some production studies of Ir-192 in literature by Langille et al. [3], Szelecsényi et al. [4], Tarkanyi et al. [5], and Hilger et al. [2]. These studies mainly intensify the production of Ir-192 on enriched Os-192 targets via (p, n) reaction processes, and the measurement by Tarkanyi et al. [5] only was a different reaction process, including  $^{192}\text{Os}(d, 2n)^{192}\text{Ir}$  together with isomeric states,  $^{192m1} + ^g\text{Ir}$ . The production of Ir-192 is also available for different methods such as the (neutron, gamma) reaction process in nuclear reactors [2, 5–7]. However, there are six stable isotopes of Os in nature, namely, Os-184 (0.02%), Os-187 (1.96%), Os-188 (13.24%), Os-189 (16.15%), Os-190 (26.26%), and Os-192 (40.78%) [8].

Therefore, in addition to  $^{192}\text{Os}(p, n)^{192}\text{Ir}$  reaction, we take into account induced reactions with deuteron, triton, helium-3, and alpha particles in the energy range between 1 MeV and 100 MeV [9–13]. Furthermore, we calculated and simulated the production of Ir-192 on Os-192, Os-189, and Os-190 targets for each charged particle. The cross-section and the integral yield calculations were performed by TALYS 1.9 code [14] and X-PMSP 2.0 program [12, 15–18], which is used to obtain the mass stopping power results of Os for the charged particles. The activities and the yield of products of reaction processes were carried out under certain circumstances, such as current beam of 1  $\mu\text{A}$  and irradiation time of 1 h. The calculated results were compared with the experimental data obtained from Exfor database [19] and other works in the literature. It is obvious that the obtained data are important to determine the production of Ir-192 in terms of other targets and the charged particle-induced reactions due to providing new nuclear data for its production.

## 2. Materials and methods

Here, we have investigated the production of radioisotope Ir-192 used in brachytherapy through nuclear reaction processes on enriched stable Os target isotopes. For this aim, we calculated the cross-section and the integral yield curves in  $E_{\text{particle}} = 100 \rightarrow 1$  MeV energy region for each reaction process. Moreover, the activities and yields of product of reaction processes as a function of irradiation time are simulated under certain conditions via TALYS 1.9 code. Besides proton-induced reaction, the radioisotope Ir-192 can be produced by deuteron, triton, helium-3, and alpha particles accelerated by particle accelerators on natural Os targets in 1–100 MeV energy range.

To produce Ir-192 on osmium targets ( $^{189,190,192}\text{Os}$ ), we followed out all reaction processes under certain situations to estimate integral yield, activity, and yield of product curves for the charged particle-induced reactions based on incident particle energy region between 1 MeV and 100 MeV. We assumed the purity of osmium targets as being above 99%, the target areas are about 1  $\text{cm}^2$ , and the target thicknesses are of uniform density during the irradiation processes in reactions. Moreover, the effective thicknesses of targets can change from 0.065 ( $^{189}\text{Os}$  for alpha-induced reaction) cm to 0.704 ( $^{192}\text{Os}$  for proton-induced reaction) as dependent on reaction process. For each reaction process, the produced heat in targets is about 0.099 kW, and the density of target materials is 22.600  $\text{g}/\text{cm}^3$ .

Furthermore, the target materials are bombarded by charged particles accelerated in particle accelerator with beam current of 1  $\mu\text{A}$  during irradiation time of 1 h in energy region  $E_{\text{particle}} = 100 \rightarrow 1$  MeV, and the cooling time is in 24 h. All the reaction processes never involve loss in activity and yield during irradiation time. The activities, yields of product, and integral yields are performed by conditions mentioned above.

The process shows that when the Os targets are bombarded by the charged particles accelerated in particle accelerators, the residual nuclei are made up, and it turns into Pt\* and Ir\* (\* means compound nucleus) isotopes by emitting different particles in very small time interval, and afterwards, the radioisotope Ir-192 is formed. Therefore, the nuclear structure properties of Pt and Ir isotopes in nuclear reaction process are also calculated such as proton, deuteron, and triton separation energies. To determine neutron ( $S_n$ ), proton ( $S_p$ ), deuteron ( $S_d$ ), and triton ( $S_t$ ) separation energies of Pt and Ir isotopes, we exploited TALYS code 1.9, which included different theoretical [20, 21] experimental tables [22] and Duflo-Zuker mass formula [14] to calculate the mass values of nuclei.

Based on reaction processes used in this work, PEQ reaction mechanism can be suitably explained by two-component exciton model which can make distinction of particle (p) and hole (h) pairs in reaction flow, besides neutron ( $\nu$ ) and proton ( $\pi$ ) particles [14]:

$$\frac{d\sigma_k^{PE}}{dE_k} = \sigma^{CF} \sum_{p_\pi=p_\pi^0}^{p_\pi^{max}} \sum_{p_\nu=p_\nu^0}^{p_\nu^{max}} W_k(p_\pi, h_\pi, p_\nu, h_\nu, E_k) \tau(p_\pi, h_\pi, p_\nu, h_\nu) \times P(p_\pi, h_\pi, p_\nu, h_\nu) \quad (1)$$

where  $\sigma^{CF}$ ,  $P$ ,  $\tau$ , and  $W_k$  are compound formation cross-section, pre-equilibrium population, mean lifetime, and emission rate, respectively. It is important to understand the estimation of particle emission situations which is available if the exciton number equals to three ( $n = 2p1h$ ) minimally. On the other hand, for an ejectile  $k$ , the emission rate  $W_k$  as dependent on two-component particle hole state density,  $\omega$  is given by [14, 23, 24]

$$W_k(p_\pi, h_\pi, p_\nu, h_\nu, E_k) = \frac{2s_k + 1}{\pi^2 3} \mu_k E_k \sigma_{k,inv}(E_k) \times \frac{\omega(p_\pi - Z_k, h_\pi, p_\nu - N_k, h_\nu, E^{tot} - E_k)}{\omega(p_\pi, h_\pi, p_\nu, h_\nu, E^{tot})} \quad (2)$$

where  $\sigma_{k,inv}(E_k)$ ,  $Z_k$ ,  $\mu_k$ , and  $s_k$  are the inverse cross-section, the charge number of the ejectile, the relative mass, and spin, respectively. Additionally, the  $\omega$  in Eq. (2) is given by single-particle state densities ( $g_\pi, g_\nu$ ) [24, 25]:

$$\omega(p_\pi, h_\pi, p_\nu, h_\nu, E_x) = \frac{g_\pi^{n_\pi} g_\nu^{n_\nu}}{p_\pi! h_\pi! p_\nu! h_\nu! (n-1)!} (U - A(p_\pi, h_\pi, p_\nu, h_\nu))^{n-1} \times f(p, h, U, V) \quad (3)$$

where  $f$ ,  $P_{p,h}$ , and  $A$  represent the finite well function, Fu's pairing function, and the Pauli correction as seen in Eqs. 4–6 and  $U = E_x - P_{p,h}$  [26]:

$$P_{p,h} = \Delta - \Delta \left[ 0.996 - 1.76 \left( \frac{n}{n_{crit}} \right)^{1.6} / \left( \frac{E_x}{\Delta} \right)^{0.68} \right]^2 \quad (4)$$

Eq. (4) is valid if  $E_x/\Delta \geq 0.716 + 2.44 \left( \frac{n}{n_{crit}} \right)^{2.17}$ ; otherwise Eq. (4) equals to  $\Delta$ .

$$A(p_\pi, h_\pi, p_\nu, h_\nu) = \frac{[\max(p_\pi, h_\pi)]^2}{g_\pi} + \frac{[\max(p_\nu, h_\nu)]^2}{g_\nu} - \frac{p_\pi^2 + h_\pi^2 + p_\nu + h_\pi}{4g_\pi} - \frac{p_\nu^2 + h_\nu^2 + p_\pi + h_\nu}{4g_\nu} \quad (5)$$

$$f(p, h, E_x, V) = 1 + \sum_{i=1}^h (-1)^i \binom{h}{i} \left[ \frac{E_x - iV}{E_x} \right]^{n-1} \Theta(E_x - iV) \quad (6)$$

where  $\Theta$  and  $V$  in the finite well function are unit step function and the potential well depth [27, 28].

### 3. Results and discussions

Based on charged particle-induced reaction processes, the production of Ir-192 on  $^{189,190,192}\text{Os}$  target materials via particle accelerator in energy region between 1 MeV and 100 MeV, we investigated the cross-section calculations (**Figure 1**), the activity (**Figure 2**), and the yield of product (**Figure 3**) curves for all the reaction processes, as well as the separation energies (**Figure 4**). Additionally, the integral yield results are calculated by data of the cross-section calculations in **Figure 1** and mass stopping power results in **Figure 5** obtained from X-PMSP 2.0 program. The separation energies in **Figure 4** are calculated to understand particle emissions that divide from residual nuclei ( $^{191,192,193,194,195}\text{Ir}^*$  and  $^{192,193,194,195,196}\text{Pt}^*$ ), which is composed of bombardment of Os target.

#### 3.1 Cross-section calculations for the production of Ir-192

To produce Ir-192, the cross-section curves with proton-, deuteron-, triton-, he-3-, and alpha-induced reactions on  $^{189,190,192}\text{Os}$  targets are presented by **Figure 1** in 1–100 MeV energy range together with experimental data by Szelecsényi et al. [4], Tarkanyi et al. [5], and Hilgers et al. [2]. The measurements by Szelecsényi et al. [4] and Hilgers et al. [2] were only performed by proton-induced reaction on Os-192 target up to 66 MeV. On the other hand, the data reported by Tarkanyi et al. [5] reaches 20 MeV deuteron incident energy only on Os-192 target. It is obvious

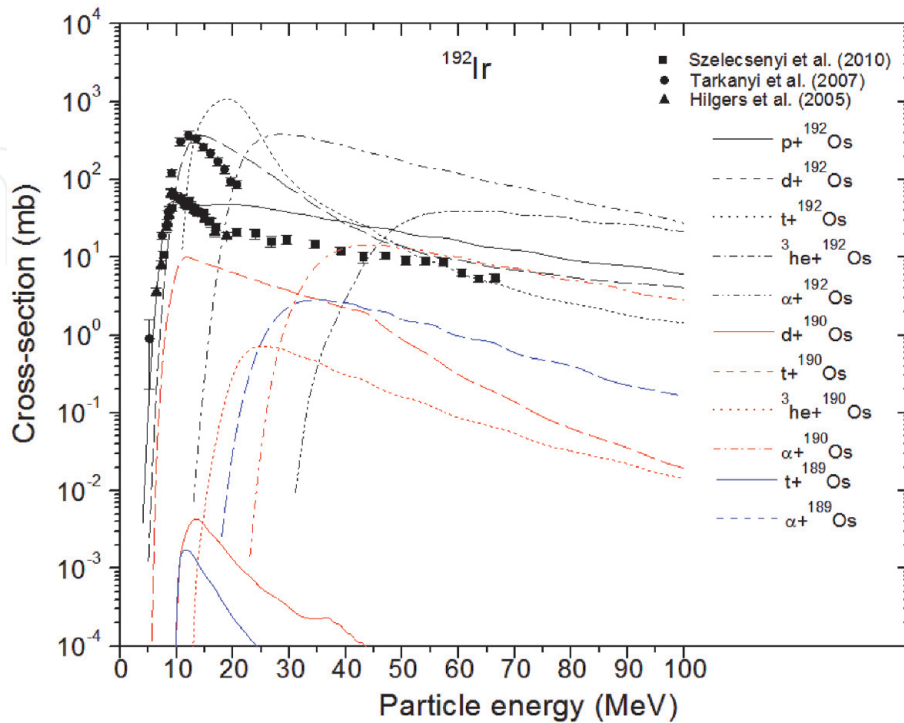


**Figure 1.**  
Cross-section curves for the production of Ir-192.



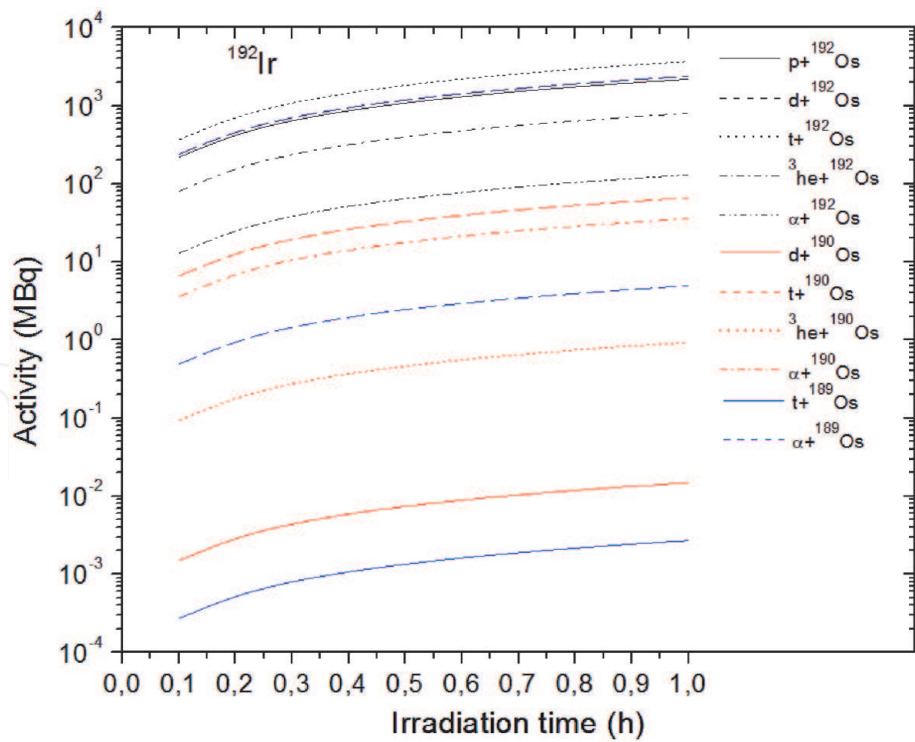


**Figure 2.**  
Activity curves for the production of Ir-192 as a function of irradiation time.

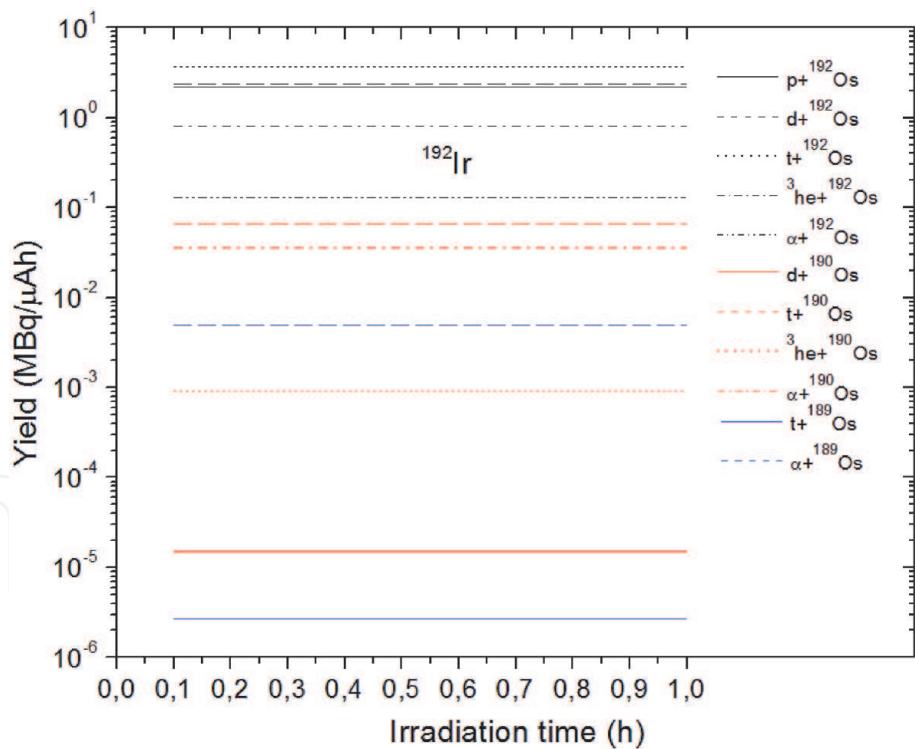


**Figure 3.**  
Yield of product curves for the production of Ir-192 as a function of irradiation time.

that the production of Ir-192 for the triton-, he-3-, and alpha-induced reactions Os-192 target does not involve any experimental result or theoretical result. In addition to Os-192 target, for Os-190 and Os-189 targets, unfortunately, the cross-section results for the production of Ir-192 are not come across different works. In comparisons of the calculated cross-section and the experimental data for Os-192 target, the theoretical result for proton-induced reaction is consistent with that of Szelecsényi et al. [4] and Hilgers et al. [2] from threshold energy to the maximum

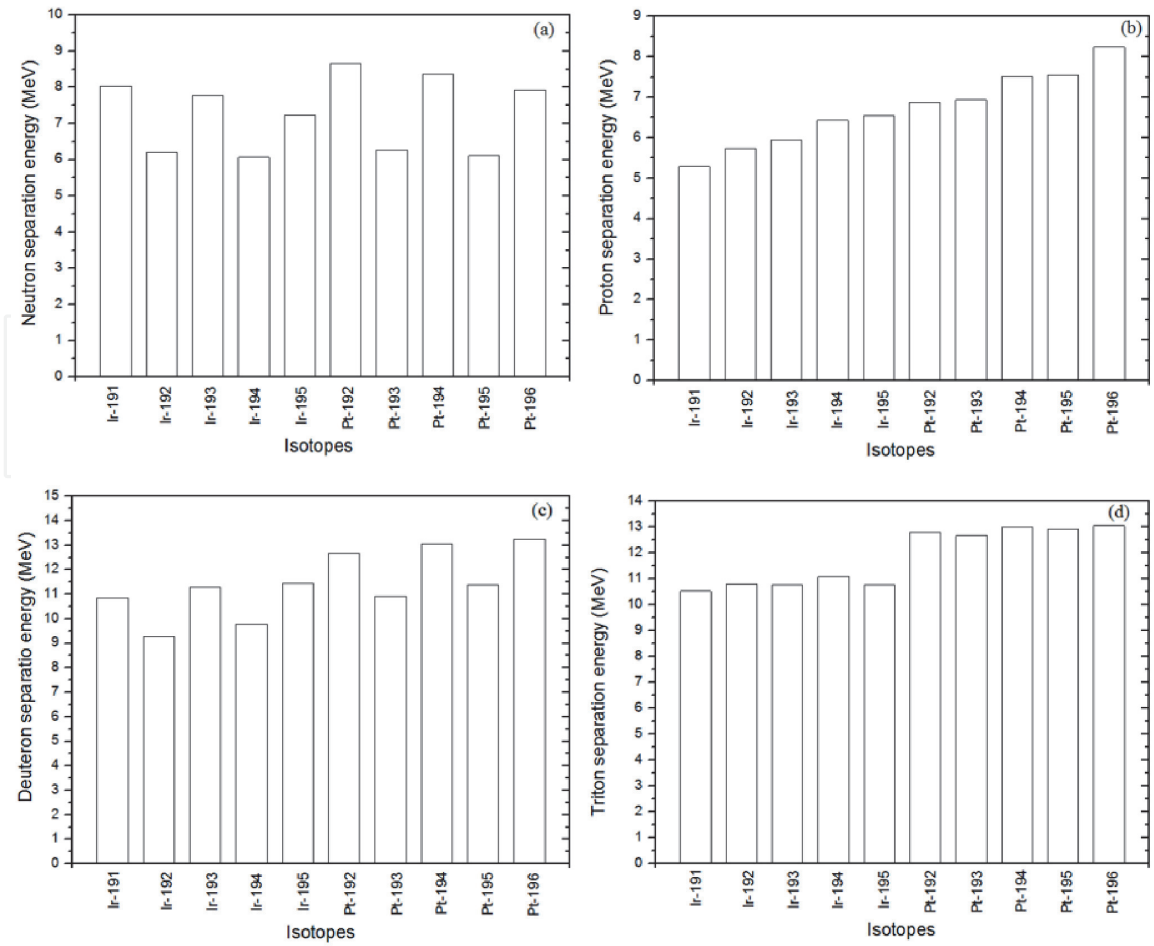


**Figure 4.**  
Calculation of separation energies for some Ir and Pt isotopes in reaction process.

cross-section value. Thus, we can conclude that the theoretical cross-section curves are consistent with the experimental data up to the highest value of cross-section curves. Moreover, the data reported by Tarkanyi et al. [5] are generally in good agreement with theoretical result up to 11 MeV deuteron incident energy. Besides proton- and deuteron-induced reaction on Os-192 target, it is important to note here that the cross-section values of the other induced reactions are suitable to obtain the radioisotope because while the maximum cross-section values for proton- and deuteron-induced reactions reach  $\sim 54$  mb and  $\sim 371$  mb at 9 MeV and 14 MeV, the cross-section values of the triton-, he-3-, and alpha-induced reactions ramp up to  $\sim 1100$  mb,  $\sim 383$  mb, and  $\sim 40$  mb at 19 MeV, 29 MeV, and 59 MeV, respectively. Furthermore, for Os-189 and Os-190 targets, alpha-induced reactions are clearly suitable compared to the other reaction types.

The results show that the production of the radioisotope Ir-192 can be produced by triton-, he-3-, and alpha-induced reactions, in addition to proton- and deuteron-induced reactions, and such productions are valid in less energy than that of 100 MeV. Therefore, to well understand the production of Ir-192 for each reaction process, we estimated activity and yield curves as a function of irradiation time by simulating under certain conditions.

### 3.2 Simulation of activity and yield of product for the production of Ir-192

The calculated cross-section results are in good agreement with the available experimental data in the literature. The reaction processes are simulated to determine the activity and yield of product curves for the production of Ir-192 as shown

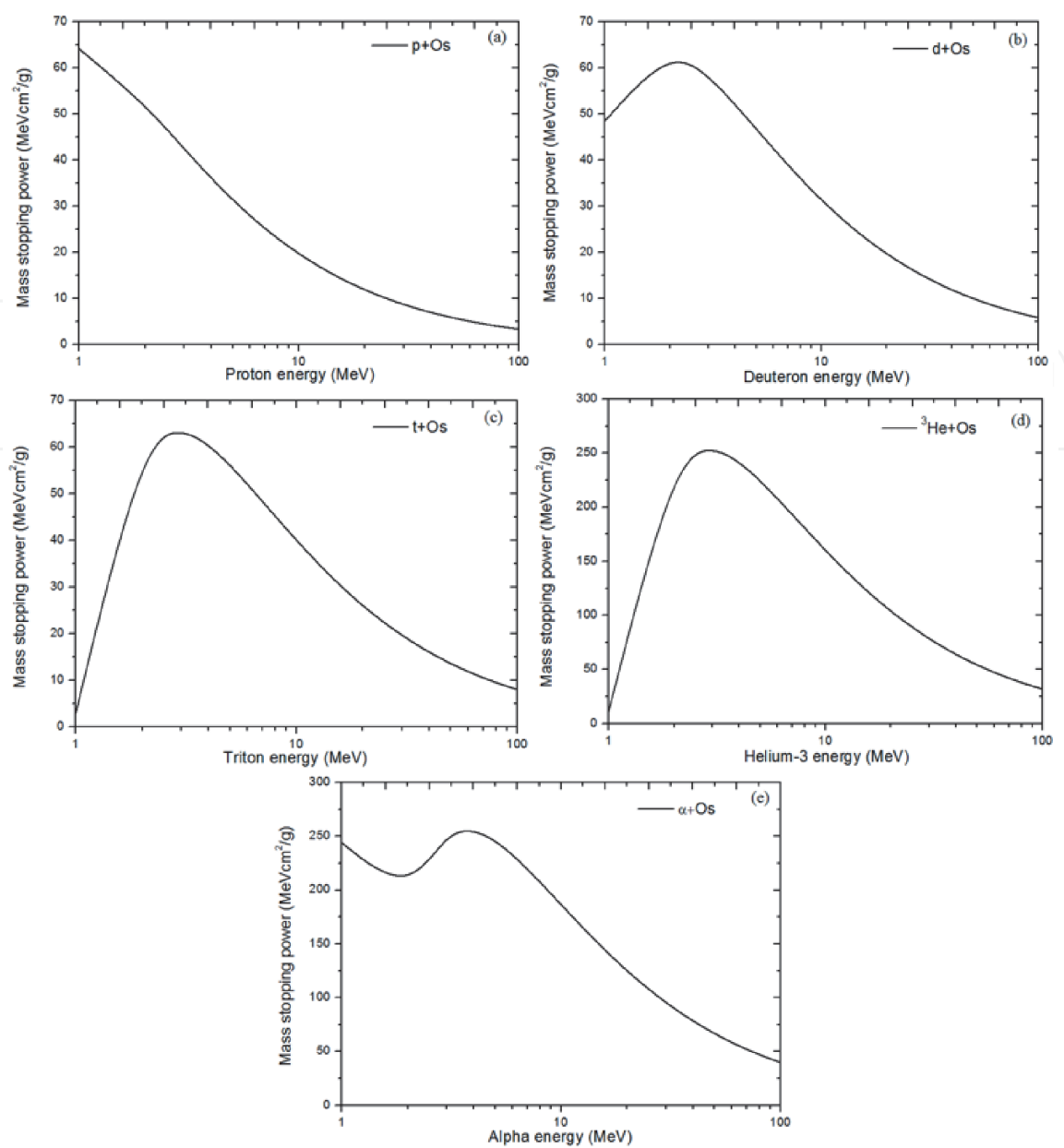


**Figure 5.**  
*Mass stopping power for the charged particles on Os target.*

in **Figures 2 and 3**. When compared with the cross-section curves, the activity and yield of product results are consistent with the cross-section curves. For Os-192 target, at end of irradiation time, the triton-induced reaction has the highest activity value of 3690 MBq. The deuteron- and proton-induced reaction reach almost the same activity values, such as 2390 MBq and 2190 MBq, respectively. On the other hand, helium-3- and alpha-induced reaction processes also have high activity values, 803 MBq and 130 MBq.

It is clear that the proton- and deuteron-induced reactions have higher activity and yield values than those of alpha- and he-3-induced reactions; however, this can be an advantage rather than disadvantage. Ir-192 is a radioisotope for brachytherapy especially for vitals, and it is used inside the capsule which is settled next to the tumor region to burn out cancerous tissues, and the radioisotope with Ir-192 high activity can bring about harm for healthy tissues. Therefore, the reaction processes with the alpha and he-3 particles can be more suitable in terms of application to patients compared to the production of Ir-192 with proton- and deuteron-induced reactions.



In addition to the production of Ir-192 on Os-192 target via the charged particle-induced reactions, when considered Os-190 and Os-189 targets, the alpha-induced reactions for both targets give suitable activity values, 35.9 MBq and 4.92 MBq, respectively. Moreover, the activity value of triton-induced reaction on Os-190 target also reaches 66.2 MBq; however, it is obvious that the triton-induced reaction on Os-189 target is insufficient. Unfortunately, it is important to say that we do not recommend the radioisotope production with triton-induced reactions due to expensive obtaining of triton. Therefore, for the production of Ir-192 on Os-190 and Os-189 targets, we can dependably propose the alpha-induced reaction process.

### 3.3 Calculation of separation energies

When the  $^{189,190,192}\text{Os}$  targets are bombarded by proton, deuteron, triton, helium-3, and alpha particles accelerated by particle accelerator, new excited compound nuclei,  $^{191,192,193,194,195}\text{Ir}$  and  $^{192,193,194,195,196}\text{Pt}$  may be made up, and after then too very while, these excited nuclei turn into new residual nuclei by emitting particles such as proton, neutron, deuteron, etc.

One of the residual nuclei also is the radioisotope Ir-192; however, there are different ways to produce Ir-192, for example, the compound nucleus Ir-193 changes to Ir-192 by emitting a neutron, and if the compound nucleus Pt-193 spreads out a proton or the Pt-194 emits a deuteron, then the radioisotope Ir-192 may be produced. Therefore, to form Ir-192 on  $^{189,190,192}\text{Os}$  targets, we calculated the separation energies of possible compound nuclei as shown in **Figure 4**. When considering the calculated separation energies for isotopes of Pt, they are higher than those of the isotopes of Ir. The he-3 and alpha separation energies are not added due to the formation of Pt and Ir isotopes in reaction processes via the charged particles. Moreover, it is obvious that the neutron separation and proton separation energies are lower than those of the other separation energies.

### 3.4 Calculation of integral yield of reaction processes

To peruse the production of Ir-192 on  $^{189,190,192}\text{Os}$  targets for the charged particle-induced reactions in energy region between 1 MeV and 100 MeV, we calculated the integral yield results of each reaction process via the calculated cross-section results in **Figure 1** and the stopping powers of Os for the charged particles obtained from X-PMSP 2.0 program (**Figure 5**); the obtained integral yield curves are presented in **Figure 6** as a function of particle energy. Based on the simulation conditions of activity and yield of product of reaction processes, the integral yield calculations were carried through in irradiation time of 1 h and a constant beam current of 1  $\mu\text{A}$ . The calculated integral yield curves were taken by the optimization of a production route into account by providing high radionuclidic purity of the Ir-192, including minimum impurity level and maximum yield value of the product.

When taking into account the nuclear reaction processes on Os-192 target, it is clearly stated that the proton-induced reaction has only experimental yield data reported by Szelecsényi et al. [4] up to 30 MeV incident proton energy. The calculated integral yield curve for proton-induced reaction is generally consistent with measurement by Szelecsényi et al. [4], up to  $\sim 15$  MeV; however, beyond 15 MeV, there is a little bit of difference when compared to the theoretical result. The reason of such a distinction is why there is difference of both theoretical and experimental cross-section curves in **Figure 1** and the error rates in the theoretical calculations and the experimental processes. Even the theoretical integral yield curve is close to the experimental data, and in terms of analyzing accuracy of the integral yield

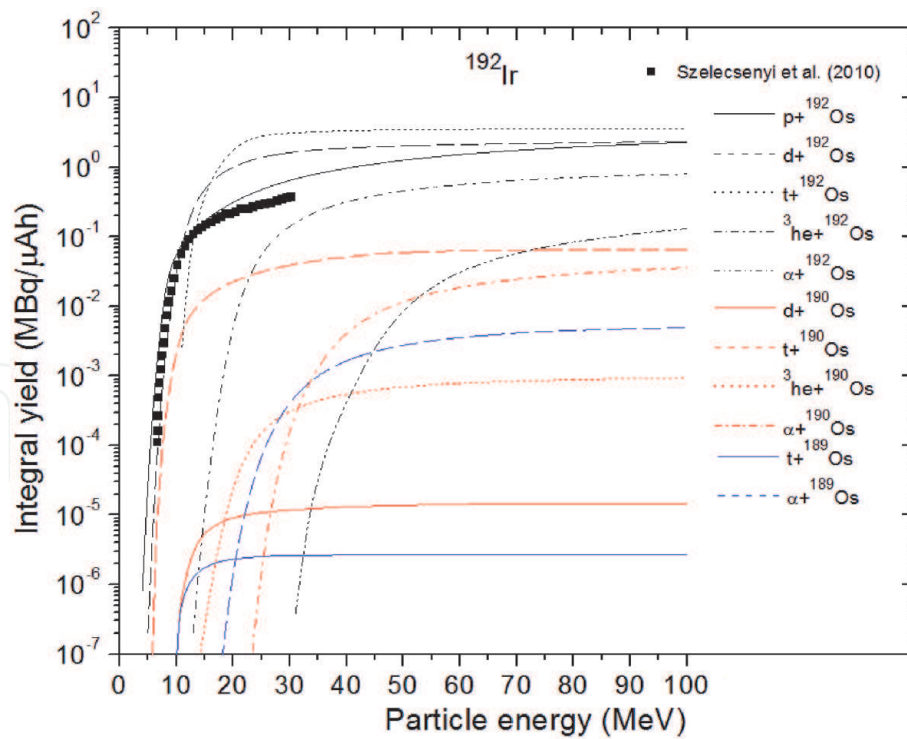


**Figure 6.**  
 Integral yield curves for the production of Ir-192 as a function of incident particle energy.

curves, it can clearly be said that the results are believable and dependable. On the other hand, the other induced reactions to produce Ir-192 are suitable, especially for deuteron- and triton-induced reactions which are of higher integral yield values (2 MBq/μAh and 4 MBq/μAh) than the proton-induced reaction (1 MBq/μAh) behind 30 MeV. Moreover, the He-3 induced reaction process gives good results; however, its appropriate energy range reaches to higher energy compared to the other induced reactions, and the alpha-induced reaction has the highest energy range to produce Ir-192.

Furthermore, based on the theoretical results, it is important to note here that while the energy range for the production of Ir-192 through proton-induced reaction can be determined as 20 → 8 MeV, the appropriate energy ranges of triton- and deuteron-induced reactions are 22 → 12 MeV and 21 → 9 MeV, respectively. These energy ranges can be formed higher than 70% of the radioisotope Ir-192; however, in these energy ranges, the contaminations in the production of Ir-192 would be brought about. The production of Ir-192 in proton-induced reactions can include the contamination of the radioisotope Ir-190 higher than 16 MeV incident proton energy. From the point of view of Szelecsenyi et al. [4], such a circumstance is valid, they pointed out that the contamination of Ir-190 for proton-induced reaction reaches 70% at 17 MeV, and unfortunately, the <sup>190</sup>Ir/<sup>192</sup>Ir activity ratio keeps up fairly high [4]. On the other hand, the production of Ir-192 on Os-190 and Os-189 targets are also presented in **Figure 6** as a function of particle energy. For Os-190 target, the triton reaction and alpha-induced reactions are more suitable than those of the other reactions. The alpha reaction process gives the best integral yield result for Os-189 target.

#### 4. Conclusion

This paper mainly investigated the production of Ir-192 used in brachytherapy via <sup>189,190,192</sup>Os targets bombarded by proton, deuteron, triton, helium-3, and alpha

particles accelerated in particle accelerators, instead of its production in nuclear reactors. Therefore, we calculated the cross-section curves and simulated activities and yields of product of all reaction processes. Additionally, to determine the energy ranges for the formation of Ir-192 in nuclear reaction processes, we estimated the integral yield results for each reaction process in energy region between 1 MeV and 100 MeV.

The calculated data were compared with the experimental data in the literature, and the obtained results for proton-induced reaction on Os-192 target showed that the theoretical results were in good agreement with available experimental data based on the cross-section and the integral yield results. When taking conformity of proton-induced reaction results into account, it is important to note here that the obtained data in this work put dependable results for the production of Ir-192 forward the literature. Because, in addition to proton-induced reaction, the obtained data for the production of Ir-192 contributes to the literature in terms of deuteron-, triton-, helium-3-, and alpha-induced reaction processes. Moreover, the calculations and simulations were also performed by charged induced reaction processes on Os-190 and Os-189 targets besides Os-192 target.

Based on the obtained results, in addition to the production of proton-induced reaction on Os-192 target, it can be said that deuteron-, triton-, helium-3-, and alpha-induced reaction on Os-192 target are suitable to produce Ir-192 in energy region between 1 MeV and 100 MeV. These energy ranges for the production of Ir-192 irrespective of contamination of the other product in the reaction processes can be given for proton-, deuteron-, triton-, he-3-, and alpha-induced reactions:  $20 \rightarrow 8$  MeV,  $21 \rightarrow 9$  MeV,  $22 \rightarrow 12$  MeV,  $35 \rightarrow 19$  MeV, and  $65 \rightarrow 34$  MeV, respectively. Furthermore, in the case of Os-190 target, the triton reaction and alpha-induced reactions are suitable compared to the other reactions, and the energy ranges are given as  $20 \rightarrow 7$  MeV and  $55 \rightarrow 25$  MeV. For Os-189 target, the alpha-induced reaction process can be proposed for the production of Ir-192 in energy range  $50 \rightarrow 21$  MeV.


## Author details

Ozan Artun

Department of Physics, Zonguldak Bülent Ecevit University, Zonguldak, Turkey

\*Address all correspondence to: ozanartun@beun.edu.tr; ozanartun@yahoo.com

## IntechOpen

© 2020 The Author(s). Licensee IntechOpen. This chapter is distributed under the terms of the Creative Commons Attribution License (<http://creativecommons.org/licenses/by/3.0>), which permits unrestricted use, distribution, and reproduction in any medium, provided the original work is properly cited. 

## References

- [1] Ghiassi-Nejad M, Jafarizadeh M, Ahmadian-Pour MR, Ghahramani AR. Dosimetric characteristics of  $^{192}\text{Ir}$  sources used in interstitial brachytherapy. *Applied Radiation and Isotopes*. 2001;**55**:189-195
- [2] Hilgers K, Sudar S, Qaim SM. Experimental study and nuclear model calculations on the  $^{192}\text{Os}[p,n]^{192}\text{Ir}$  reaction: Comparison of reactor and cyclotron production of the therapeutic radionuclide  $^{192}\text{Ir}$ . *Applied Radiation and Isotopes*. 2005;**63**:93-98
- [3] Langille G, Yang H, Zeisler SK, Hoeher C, Storr T, Andreoiu C, et al. Low energy cyclotron production and cyclometalation chemistry of iridium-192. *Applied Radiation and Isotopes*. 2016;**115**:81-86
- [4] Szelecsényi F, Vermeulen C, Steyn GF, Kovács Z, Aardaneh K, van der Walt TN. Excitation functions of  $^{186,187,188,189,190,192}\text{Ir}$  formed in proton-induced reactions on highly enriched  $^{192}\text{Os}$  up to 66 MeV. *Nuclear Instruments and Methods B*. 2010;**268**:3306-3314
- [5] Tarkanyi F, Hermanne A, Takacs S, Hilgers K, Kovalev SF, Ignatyuk AV, et al. Study of the  $^{192}\text{Os}[d,2n]$  reaction for production of the therapeutic radionuclide  $^{192}\text{Ir}$  in no-carrier added form. *Applied Radiation and Isotopes*. 2007;**65**:1215-1220
- [6] Ananthakrishnan M. Iridium 192. In: *Manual for Reactor Produced Radioisotopes IAEA-TECDOC-1340*. 2003. p. 116. Available from: [https://www.pub.iaea.org/MTCD/Publications/PDF/te\\_1340\\_web.pdf](https://www.pub.iaea.org/MTCD/Publications/PDF/te_1340_web.pdf) [Accessed: 02 January 2020]
- [7] Schaeken B, Vanneste F, Bouiller A, Hoornaert MT, Vandenbroeck S, Hermans J, et al.  $^{192}\text{Ir}$  brachytherapy sources in Belgian hospitals. *Nuclear Instruments and Methods A*. 1992;**312**:251-256
- [8] NIST, National Institute of Standards and Technology. 2018. Available from: <https://www.nist.gov/> [Accessed: 02 January 2020]
- [9] Artun O. Calculation of productions of PET radioisotopes via phenomenological level density models. *Radiation Physics and Chemistry*. 2018;**149**:73-83
- [10] Artun O. Investigation of the productions of medical  $^{82}\text{Sr}$  and  $^{68}\text{Ge}$  for  $^{82}\text{Sr}/^{82}\text{Rb}$  and  $^{68}\text{Ge}/^{68}\text{Ga}$  generators via proton accelerator. *Nuclear Science and Techniques*. 2018;**29**:137-147
- [11] Artun O. Investigation of the production of cobalt-60 via particle accelerator. *Nuclear Technology & Radiation Protection*. 2017;**32**(4):327-333
- [12] Artun O. Estimation of the production of medical Ac-225 on thorium material via proton accelerator. *Applied Radiation and Isotopes*. 2017;**127**:166-172
- [13] Artun O. Investigation of the production of promethium-147 via particle accelerator. *Indian Journal of Physics*. 2017;**91**:909-914
- [14] Koning A, Hilaire S, Goriely S. *Talys Manual 1.9*. 2017. Available from: <http://www.talys.eu/download-talys/> [Accessed: 02 January 2020]
- [15] Artun O. Calculation of the mass stopping powers of medical, chemical, and industrial compounds and mixtures. *Nuclear Technology & Radiation Protection*. 2018;**33**(4):356-362
- [16] Artun O. X-particle the mass stopping. In: *Power, X-PMSP*



Version 2.00. 2018. Available from: <https://www.x-pmsp.com/> [Accessed: 02 January 2020]

[17] Artun O. Calculation of productions of medical  $^{201}\text{Pb}$ ,  $^{198}\text{Au}$ ,  $^{186}\text{Re}$ ,  $^{111}\text{Ag}$ ,  $^{103}\text{Pd}$ ,  $^{90}\text{Y}$ ,  $^{89}\text{Sr}$ ,  $^{77}\text{Kr}$ ,  $^{77}\text{As}$ ,  $^{67}\text{Cu}$ ,  $^{64}\text{Cu}$ ,  $^{47}\text{Sc}$  and  $^{32}\text{P}$  nuclei used in cancer therapy. *Applied Radiation and Isotopes*. 2019;**144**:64-79

[18] Artun O. Investigation of production of samarium-151 and europium-152,154,155 via particle accelerator. *Modern Physics Letters A*. 2019;**33**:1950154

[19] Exfor. Available from: <https://www.nds.iaea.org/exfor/exfor.htm>; 2019

[20] Goriely S, Pearson JM. Skyrme-Hartree-Fock-Bogoliubov nuclear mass formulas: Crossing the 0.6 MeV accuracy threshold with microscopically deduced pairing. *Physical Review Letters*. 2009;**102**:152503

[21] Möller P, Nix JR, Myers WD, Swiatecki WJ. Nuclear ground-state masses and deformations. *Atomic Data and Nuclear Data Tables*. 1995;**59**: 185-381

[22] Wapstra AH, Audi G, Thibault C. The Ame2003 atomic mass evaluation: I. evaluation of input data, adjustment procedures. *Nuclear Physics A*. 2003;**729**:129-336

[23] Cline CK, Blann M. The pre-equilibrium statistical model: Description of the nuclear equilibration process and parameterization of the model. *Nuclear Physics A*. 1971;**172**: 225-229

[24] Dobes J, Betak E. Two-component exciton model. *Zeitschrift für Physik*. 1983;**310**:329-338

[25] Betak E, Dobes J. The finite depth of the nuclear potential well in the exciton model of preequilibrium decay.

*Zeitschrift für Physik A*. 1976;**279**: 319-324

[26] Fu CY. Implementation of on advanced pairing correction for particle-hole state densities in precompound nuclear reaction theory. *Nuclear Science and Engineering*. 1984;**86**:344-354

[27] Kalbach C. Surface and collective effects in preequilibrium reactions. *Physical Review C*. 2000;**62**:44608

[28] Kalbach C. Surface effects in the exciton model of preequilibrium nuclear reactions. *Physical Review C*. 1985;**32**: 1157